ACS APPLIED MATERIALS & INTERFACES

Research Article

www.acsami.org

Phenolphthalein-based Poly(arylene ether sulfone nitrile)s Multiblock Copolymers As Anion Exchange Membranes for Alkaline Fuel Cells

Ao Nan Lai, Li Sha Wang, Chen Xiao Lin, Yi Zhi Zhuo, Qiu Gen Zhang,* Ai Mei Zhu, and Qing Lin Liu*

Department of Chemical & Biochemical Engineering, Fujian Provincial Key Laboratory of Theoretical and Computational Chemistry, The College of Chemistry and Chemical Engineering, Xiamen University, Xiamen 361005, People's Republic of China

Supporting Information

ABSTRACT: A series of phenolphthalein-based poly(arylene ether sulfone nitrile)s (PESN) multiblock copolymers containing 1−methylimidazole groups (ImPESN) were synthesized to prepare anion exchange membranes (AEMs) for alkaline fuel cells. The ion groups were introduced selectively and densely on the unit of phenolphthalein as the hydrophilic segments, allowing for the formation of ion clusters. Strong polar nitrile groups were introduced into the hydrophobic segments with the intention of improving the dimensional stability of the AEMs. A well-controlled multiblock structure was responsible for the well-defined hydrophobic/hydrophilic phase separation and interconnected ion−transport channels, as confirmed by atomic force microscopy and small angle X-ray scattering. The ImPESN membranes with low swelling showed a relatively high water uptake, high hydroxide ion conductivity together with good mechanical, thermal and alkaline stability. The ionic conductivity of the membranes was in the range of 3.85−14.67 × 10^{-2} S·cm^{-1} from 30 to 80 °C. Moreover, a single H_2/O_2 fuel cell with the ImPESN membrane showed an open circuit voltage of 0.92 V and a maximum power density of 66.4 mW cm^{-2} at 60 °C.

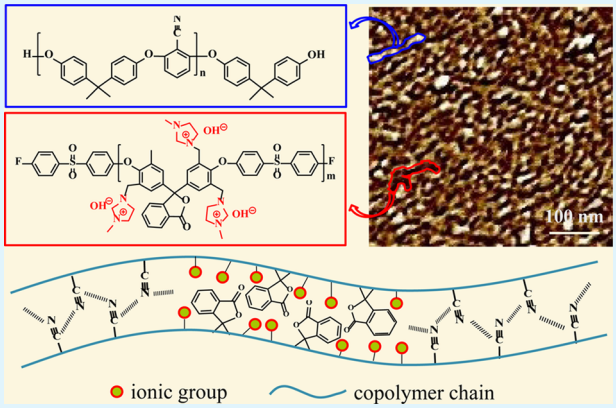

KEYWORDS: *anion exchange membrane, alkaline fuel cells, poly(arylene ether sulfone nitrile), multiblock copolymer, phenolphthalein*

1. INTRODUCTION

As one of the most promising power sources, polymer electrolyte fuel cells (PEFCs) have currently drawn great attention due to their high energy efficiency, low cost, and environmental friendliness.[1,2] Of various types of PEFCs, proton exchange membrane fuel cells (PEMFCs) are the most widely investigated ones. Perfluorosulfonic acid ion exchange membranes such as Nafion are commonly used as PEMs in PEMFCs, which exhibit excellent chemical resistance, high thermal, and mechanical stability, and good ionic conductivity.[3,4] Nevertheless, these advantages come with several drawbacks, such as the requirement of noble metal electro−catalysts, high cost of perfluorinated membranes, and insufficient stability of membranes under operating conditions, which impede the commercialization of PEMFCs.

Anion exchange membrane fuel cells (AEMFCs) were developed as an alternative because they have some advantages over PEMFCs, including good reaction kinetics and low overpotential for fuel oxidation, allowing for the use of non-noble metal catalysts (such as Ni and Co) and relatively high fuel cell performance.[5] In addition, the fuel for the AEMFCs is flexible (e.g., methanol, ethanol, ethylene glycol, etc.).[6] As key materials in AEMFCs, various AEMs with main chain structures such as poly(arylene ether sulfone) (PES),[7−9] poly(arylene ether ketone) (PEK),[10] poly(phenylene oxide),[11,12] and polymerized ionic liquid[13] have been reported over the years. However, the existing AEMs display insufficient conductivity or stability which limits their use for AEMFCs. Recent research has shown that, similar to PEMs, AEMs with a multiblock structure displayed well-defined hydrophilic/hydrophobic microphase separation, resulting in improved conductivity and thermal stability.[14−18]

As one of the cardo groups, phenolphthalein (PPH) contains a heterocyclic pendant lactone group. It has been integrated in polymers such as poly(arylene ether)s, polycarbonates and polyesters. Due to the bulky structure and fully aromatic, PPH has contributed significantly to the thermal stability and mechanical properties of those polymers.[19] Moreover, it is assumed that the introduction of PPH into the polymer chain could provide large free volume in membranes which is beneficial for the water molecules storing for PEMs applications.[20] Recently, the synthesis of AEMs by chloromethylation of commercial polymer phenolphthalein-based cardo PES and

Received: February 14, 2015
Accepted: March 31, 2015
Published: March 31, 2015

DOI: 10.1021/acsami.5b01475
ACS Appl. Mater. Interfaces 2015, 7, 8284−8292

PEK followed by quaternization and hydroxide exchange has been reported.[21−23] However, several obvious drawbacks of chloromethylation have limited its application. Zhang et al.[24] synthesized a series of novel side chain type phenolphthalein-based PES AEMs through modifying the lactone ring by the reaction of phenolphthalein with diamine. The flexible side chain facilitates the ion aggregation and microphase separation. However, due to the low ion group density per unit of the random ionomers, the ion cluster size was small, and the connection of the ion domains was poor in the membranes.

In this study, tetramethyl-contained phenolphthalein-based poly(arylene ether sulfone nitrile)s multiblock copolymers were systhesized. The copolymers were further treated by bromination and imidazolium functionalization to prepare a new kind of AEMs. Along these processes, the ion groups were introduced selectively and densely on the unit of phenolphthalein as the hydrophilic segments, allowing for the formation of ion channels and phase−separated structure. The introduction of strong polar nitrile groups into the hydrophobic segments was intended to improve the dimensional stability inspired by the previous studies of PEMs.[25,26] Then, the as−prepared AEMs were characterized by ^{1}H NMR and FT-IR. Their water uptake, swelling ratio, ionic exchange capacity, ionic conductivity, and thermal and alkaline stabilities were also measured. The structure−property relationship of the AEMs was studied by controlling the length of hydrophilic segment.

2. EXPERIMENTAL SECTION

2.1. Materials. Bis(4−fluorophenyl) sulfone (FPS; 99%, TCI, Japan), 2,6-difluorobenzonitrile (DFBN; 99%, Aladdin, China), 2,6-dimethylphenol (99%, Aladdin, China), phthalic anhydride (99%, Aladdin, China), methanesulfonic acid (99%, Aladdin, China), bisphenol A (BHA; 97%, Sigma-Aldrich, St. Louis, MO) and 1-methylimidazole (MIm; 99%, Aladdin, China) were used as received. Toluene and *N*,*N*-dimethylacetamide (DMAc; 99.8%, Aladdin, China) were stirred over CaH_2 for 24 h, then distilled under reduced pressure and stored over 4 Å molecular sieves. Benzoyl peroxide (BPO; 99%, Sinopharm, China) was supplied from Tianjin Guangfu Fine Chemical Research Institute (China) and recrystallized from chloroform. All other chemicals were supplied from Shanghai Sinopharm Chemical Reagent Co., Ltd. (China) and used without further purification.

2.2. Preparation of Anion Exchange Membranes. *2.2.1. Synthesis of the Monomer 3,3-Bis(4-hydroxy-3,5-dimethylphenyl)−Phenolphthalein (DMPPH).* DMPPH was synthesized from 2,6-dimethylphenol and phthalic anhydride (Scheme 1) by the method

Scheme 1. Synthesis of the Monomer DMPPH

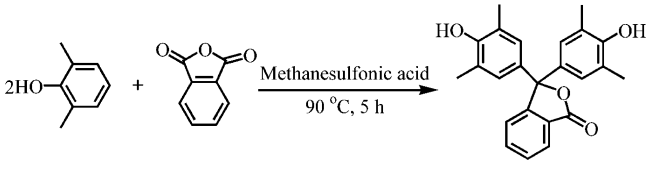

reported in the literature.[27] 2,6-Dimethylphenol (16.247 g, 0.133 mol), phthalic anhydride (10.960 g, 0.074 mol), and methanesulfonic acid (27 mL, 0.416 mol) were introduced into a 150 mL three-necked round-bottomed flask equipped with a magnetic stirrer, a thermometer, and a condenser. The reaction mixture was stirred at 90 °C for 5 h, cooled to room temperature (RT), and slowly poured into ice water to yield a precipitate. The precipitate was filtered, washed thoroughly with deionized (DI) water and toluene, and then dried at 80 °C under vacuum for 24 h to obtain the product (yield, 82%).

2.2.2. Synthesis of Fluorine-Terminated Telechelic Oligomers (Oligomer-F). A typical procedure for the synthesis of oligomer-F is detailed below (m = 19 in Scheme 2). A 100 mL three-necked round-bottomed flask equipped with a Dean−Stark trap was charged with DMPPH (3.7443 g, 10 mmol), FPS (2.6696 g, 10.5 mmol), 3.4553 g (25 mmol) of K_2CO_3, DMAc (30 mL) and toluene (15 mL). The reaction mixture was heated to 140 °C under nitrogen for 4 h and subsequently kept at 165 °C for another 12 h. At the end of the reaction, another 50 mg of FPS was introduced to ensure the end-capping. Afterward, the reaction mixture was cooled to RT and poured into 400 mL of aqueous methanol solution (DI water/methanol = 1/1, v/v) to get a precipitate. Then, the precipitate was magnetically stirred at 80 °C for another 5 h, collected by filtration, Soxhlet extracted with methanol for 12 h, and dried at 60 °C under vacuum for 48 h to yield a pale white solid product. The chemical structure of the as-synthesized oligomer-F was characterized using ^{1}H NMR. The polymerization degree of oligomer-F was determined to be m = 19 from GPC.

2.2.3. Synthesis of Hydroxy-Terminated Telechelic Oligomers (Oligomer-OH). Similar to oligomer-F, oligomer-OH was synthesized as follows (n = 22 in Scheme 2). A 100 mL three-necked round-bottomed flask equipped with a Dean−Stark trap was charged with DFBN (1.3910 g, 10 mmol), BHA (2.3970 g, 10.5 mmol), 3.4553 g (25 mmol) of K_2CO_3, DMAc (30 mL) and toluene (15 mL). The reaction was carried out to yield a viscous mixture. After the same purification and drying treatments, a pale white solid product of oligomer-OH was obtained. The chemical structure of the oligomer-OH was characterized using ^{1}H NMR. The polymerization degree of the oligomer-OH was determined to be n = 22 from GPC.

2.2.4. Synthesis of Multiblock Tetramethyl-Contained Phenolphthalein-based Poly(arylene ether sulfone nitrile)s (MPESN). A typical procedure for the synthesis of MPESN is as follows (Scheme 2). An equimolar amount of the oligomer-F (m = 19) and oligomer-OH (n = 22) was mixed with K_2CO_3 and copolymerized at 145 °C for 4 h and then at 165 °C for another 20 h under nitrogen. DMAc and toluene were also used as the solvent and azeotropic solvent in the reaction, respectively. After the polymerization, additional DMAc was added to decrease the viscosity. Then, the mixture was cooled to RT and poured into 400 mL of aqueous methanol solution (DI water/methanol = 1/1, v/v) to produce a solid precipitate. Then, the precipitate was magnetically stirred at 80 °C for another 5 h, collected by filtration, Soxhlet extracted with methanol for 12 h, and dried at 60 °C under vacuum for 48 h to yield a white solid target product of MPESN-19-22. The chemical structure and molecular weight of the as−synthesized multiblock copolymers were characterized using ^{1}H NMR and GPC.

2.2.5. Bromination of MPESN. The MPESN was benzyl brominated using *N*-bromosuccinimide (NBS) as the bromination agent and BPO as the initiator in 1,1,2,2−tetrachloroethane (TCE). A typical procedure is as follows. First, 1.0 g of MPESN-19-22 and 20 mL of TCE were added to a 100 mL three-necked round-bottomed flask and heated to 85 °C under stirring. Then, 1.185 g of NBS and 0.081 g of BPO were introduced after the copolymer dissolved completely. The bromination reaction was proceeded at 85 °C for 5 h under nitrogen. After bromination, the reaction mixture was cooled to RT and poured into 400 mL of methanol solution to produce a precipitate. Then, the precipitate was collected by filtration, Soxhlet extracted with methanol for 12 h, and dried at 60 °C under vacuum for 48 h to yield a yellow solid product of BrPESN-19-22, where Br denotes the bromination reaction.

2.2.6. Synthesis of Imidazolium Functionalized Poly(arylene ether sulfone nitrile)s (ImPESN) and Membrane Formation. ImPESN was synthesized via the nucleophilic substitution reaction of BrPESN with MIm (Scheme 2). A typical procedure was as follows. First, 1.0 g of BrPESN-19-22 and 20 mL of DMSO were added to a 50 mL round-bottomed flask and heated to 45 °C under stirring. Then, 1.1 mL of MIm was introduced slowly after the copolymer dissolved completely. The reaction solution was stirred at 45 °C for 12 h, followed by filtrating through a 0.45 μm PTFE membrane filter. The resulting solution was then cast onto a clean glass plate and heated at 60 °C under vacuum for 48 h to obtain a transparent membrane. Then, the membrane was immersed in a 1 M KOH solution at RT for 24 h to exchange with OH^- and kept in DI water for more than 24 h before use. The obtained membrane is termed ImPESN-19-22, where Im denotes the imidazolium functionalization.

DOI: 10.1021/acsami.5b01475
ACS Appl. Mater. Interfaces 2015, 7, 8284−8292

Scheme 2. Synthesis of Oligomer-OH, Oligomer-F, MPESN, BrPESN, and ImPESN

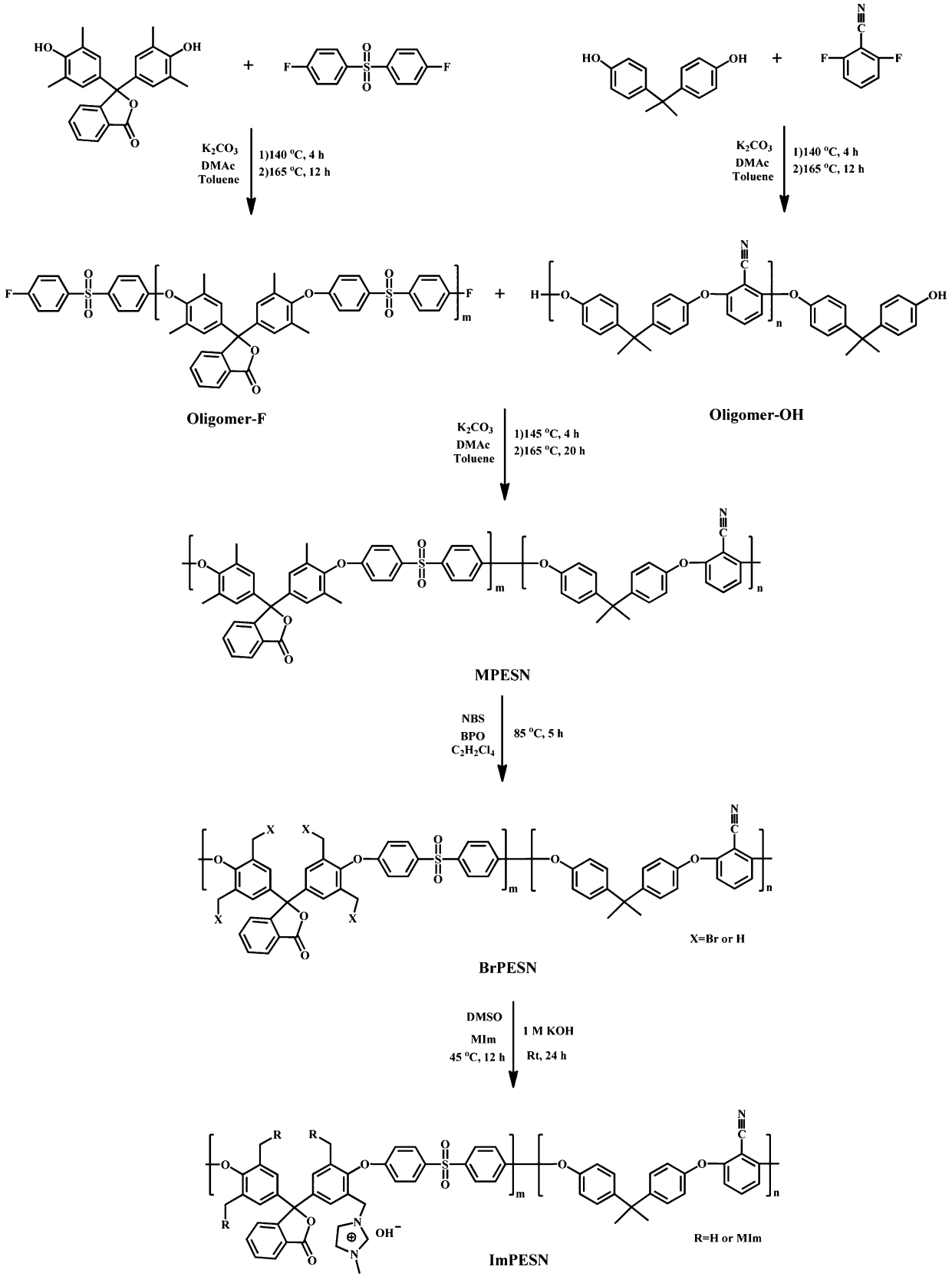

2.3. Characterization. *2.3.1. ^{1}H NMR and FT-IR Spectroscopy.* ^{1}H NMR spectra were recorded on an Avancell 500 MHz spectrometer (Bruker, Switzerland) using tetramethylsilane (TMS) as the internal standard and deuterated chloroform ($CDCl_3$) or deuterated dimethyl sulfoxide (DMSO-d_6) as the solvent. The FT-IR spectra of the polymer and AEM samples were recorded in the range of 500−4000 cm^{-1} with an accumulation of 32 scans on a Nicolet Avatar 330 spectrophotometer (Thermo Electron Corporation).

DOI: 10.1021/acsami.5b01475
ACS Appl. Mater. Interfaces 2015, 7, 8284−8292

2.3.2. GPC Measurement. The molecular weight of the sample was measured via a GPC system (Waters, Milford, MA) equipped with a Waters 1515 isocratic HPLC pump, three Styragel columns (Waters HT4, HT5E, and HT6) and a Waters 2414 refractive index detector. An HPLC-grade tetrahydrofuran (THF) was used as the eluent feeding at a flow rate of 1.0 mL·min^{-1}and polystyrene as the standard.

2.3.3. Scanning Electron Microscopy (SEM). A field emission scanning electron microscope (SEM, S−4800, Hitachi, Japan) was used to study the morphology of the membrane. Before observation, the membrane was fractured with liquid nitrogen and coated with gold.

2.3.4. Atomic Force Microscopy (AFM). The surface AFM micrographs of the AEMs was recorded on an atomic force microscopy (5500, Agilent Technologies). Tapping mode was used in the measurement under ambient condition. The membrane sample was equilibrated in 60% RH at least 24 h before testing. All the AFM phase images are shown as recorded without any extra image treatment.

2.3.5. Small Angle X-ray Scattering (SAXS). SAXS profiles of the AEMs were obtained using a SAXSess-MC2 X-ray scattering spectrometer (Anton Paar, Austria) at RT. The range of scattering wave vectors ($q = 4\pi \sin\theta/\lambda_i$) is from 0.05 to 1.0 nm^{-1}, where λ_i is the incident wavelength and θ is the half of scattering angle.

2.3.6. Ionic Exchange Capacity (IEC). The IEC of the AEMs was measured by the classical back-titration method. A dry membrane in the OH$^-$ form was soaked in a 0.1 M HCl solution for 24 h, followed by back-titrating with a 0.05 M KOH solution. The IEC (mequiv·g^{-1}) is calculated from

$$\mathrm{IEC}\ (\%) = \frac{M_{o,HCl} - M_{e,HCl}}{m_d} \times 100 \quad (1)$$

where $M_{o,HCl}$ and $M_{e,HCl}$ (mequiv) are the milliequivalents of HCl before and after equilibrium, respectively, and m_d (g) is the weight of the dry membrane.

2.3.7. Water Uptake (WU). The WU of all the membranes was determined via a quartz spring, as previously reported.[7] Before measurement, a dry membrane was obtained by drying at 60 °C under vacuum for 48 h. In the measurement, the quartz spring with an original length of L_1 was hung on a ground-glass stopper that was fixed on the top of an inner glass cylinder equipped with a sealed bottom. After a piece of the dry membrane was loaded, the quartz spring extended to a length of L_2. Then, 50 mL of DI water was added to the cylinder to generate a saturated water vapor at a given temperature. The temperature of the system was adjusted by controlling the temperature of the circulating water between the outer and the inner glass cylinders. The membrane swelled in the water vapor. After 48 h, the quartz spring extended to an ultimate length of L_3. The WU of the membrane is calculated from Hooke's law

$$\mathrm{WU}\ (\%) = \frac{kL_3 - kL_2}{kL_2 - kL_1} \times 100 = \frac{L_3 - L_2}{L_2 - L_1} \times 100 \quad (2)$$

where k is the elasticity coefficient of the quartz spring. The average number of absorbed water molecules per ion group, λ, is calculated from[16]

$$\lambda = \frac{\mathrm{WU}}{M_{H_2O}} \times \frac{1000}{\mathrm{IEC}} \quad (3)$$

where M_{H_2O} is the molecular weight of water (18.02 g mol^{-1}).

2.3.8. Swelling Ratio (SR). The SR of the membrane was investigated in the plane direction by immersing a rectangular sample into DI water and calculated from

$$SR\ (\%) = \frac{L_w \times W_w - L_d \times W_d}{L_d \times W_d} \times 100 \quad (4)$$

where L_d and L_w are the length of the dry and wet membranes, respectively, and W_d and W_w are the width of the dry and the wet membranes, respectively.

2.3.9. Ionic Conductivity. The ionic conductivity of the AEM was measured by the two-electrode AC impedance spectroscopy method using a Parstat 263 electrochemical workstation (Princeton Advanced Technology, Princeton, NJ).[7] Before testing, the OH$^-$ form membrane was kept in DI water for at least 24 h. The measurement was conducted at various temperatures with the membrane immersed in DI water in a chamber and degassed with flowing N_2 gas to exclude CO_2. The ionic conductivity (σ, S·cm^{-1}) is calculated from

$$\sigma = \frac{l}{AR} \quad (5)$$

where l (cm) is the distance between two electrodes, A (cm^2) is the cross-sectional area of the membrane, and R (Ω) is the resistance of the membrane.

2.3.10. Mechanical Property. A universal testing instrument (WDW-1E Testing System) was used to investigate the mechanical property of the membrane with a tensile speed of 10 mm·min^{-1} at RT under 60% relative humidity (RH). A 15 mm wide membrane was immersed in DI water at RT for 24 h; before testing, we removed the membrane from the water and wiped off the surface water using filter paper.

2.3.11. Thermal Stability. A thermogravimetric analyzer (TGA, SDQT600) was used to analyze the thermal stability of the membrane with a heating rate of 10 °C·min^{-1} in nitrogen. Before testing, the membrane was dried at 60 °C under vacuum for 48 h.

2.3.12. Alkaline Stability. The alkaline stability of the membrane was evaluated by soaking the OH$^-$ form membrane in a 2 M KOH solution at 60 °C to enable us to observe the change in ionic conductivity and chemical structure. Before testing, the membrane was washed with DI water for several times and kept in DI water for more than 24 h.

2.3.13. Membrane Electrode Assembly (MEA) and Single Cell Performance. The MEA with ImPESN-19-22 was made by the method as previously reported.[7] Pt/C (40 wt % Pt, Johnson Matthey) and Teflon-treated carbon paper (Toray-250) were used as the anode/cathode catalyst and diffusion layer, respectively. The catalyst and glycerol were mixed in ionomer solution (5 wt % in DMSO, obtained by dissolving a piece of the OH$^-$ form ImPESN-30-22 membrane in DMSO at RT) under ultrasonic dispersion for 15 min and magnetic stirring for 24 h to obtain a homogeneous catalyst ink. Then the catalyst ink was sprayed onto the carbon paper to prepare the anode and cathode catalyst layers. The Pt loading and ionomer content were 1 mg·cm^{-2} and 30 wt % in the catalyst layer, respectively. The effective electrode area was 4 cm^2. The MEA was fabricated by sandwiching the OH$^-$ form AEM between the cathode and anode electrodes and followed by hot-pressing at 0.8 MPa and 50 °C for 10 min. The single cell test with the MEA was carried out at 60 °C and 100% RH on an electronic load (ZY8714, ZHONGYING Electronic Co., Ltd.). During the test, the single cell was supplied with O_2 (cathode) and H_2 (anode) at a flow rate of 100 and 50 mL·min^{-1}, respectively.

3. RESULTS AND DISCUSSION

A series of tetramethyl-contained phenolphthalein-based poly(arylene ether sulfone nitrile)s multiblock copolymers (MPESN-9-22, MPESN-19-22, and MPESN-30-22) and their brominated products (BrPESN-9-22, BrPESN-19-22 and BrPESN-30-22) were synthesized via block copolymerization and bromination reaction. Their chemical structures and molecular weights were characterized by ^{1}H NMR, FT-IR, and GPC.

3.1. Synthesis and Characterization of the Monomer DMPPH. The monomer DMPPH was synthesized by reacting 2,6-dimethylphenol with phthalic anhydride in methanesulfonic acid at 90 °C for 5 h, as shown in Scheme 1. The structure was identified by ^{1}H NMR in DMSO-d6. As shown in Figure S1 (Supporting Information), the peak at 8.42 ppm is associated with hydroxyl groups, and the peak at 2.11 ppm is assignable to benzylmethyl groups. The clear peaks H_b to H_f associated with the aromatic protons confirm the structure of DMPPH.

3.2. Synthesis and Characterization of Telechelic Hydrophilic and Hydrophobic Oligomers. A series of telechelic hydrophilic oligomers and telechelic hydrophobic oligomers were synthesized via polycondensation reactions, as

DOI: 10.1021/acsami.5b01475
ACS Appl. Mater. Interfaces 2015, 7, 8284−8292

shown in Scheme 2. The chemical structure and lengths of the oligomers were determined by ^{1}H NMR (Figure S2, Supporting Information) and GPC (Table 1), respectively. Protons attached to F-terminated sulfonyl phenylene rings (g′ and h′) appeared at lower magnetic fields than those of the sulfonyl phenyleneoxy rings (g and h) because of the strong electron-withdrawing efficiency of the fluorine groups (Figure S2a, Supporting Information). Protons of OH−terminated phenylene rings (i′ and j′) appeared at higher magnetic fields than those of oxyphenylene rings (i and j) because of the strong electron-donating efficiency of the hydroxy groups (Figure S2b, Supporting Information). The degrees of polymerization were controlled at 9, 19, and 30 for oligomer-F and at 22 for oligomer-OH by adjusting the feed molar ratio of the fluorine-containing monomers to the hydroxy-containing monomers. All the results support the formation of the telechelic oligomers.

Table 1. Expected and Experimental Degree of Polymerization and Molecular Weight of Oligomers

oligomer	expected length[a]	obtained length[b]	M_n (Da)	M_w (Da)	M_w/M_n
m9	10	8.8	5207	8285	1.5911
m19	20	18.9	11136	17811	1.5994
m30	30	29.5	17374	27977	1.610
n22	20	21.9	7190	10583	1.4719

[a]Calculated value from the feed monomer ratio. [b]Determined by GPC.

3.3. Synthesis and Characterization of Block Copolymers. Three series of block copolymers with different lengths of hydrophilic segments, MPESN-9-22, MPESN-19-22 and MPESN-30-22, were prepared by the reaction of the hydrophilic oligomers (m9, m19, and m30) with the hydrophobic oligomer (n22), respectively. Figure S3a (Supporting Information) shows the ^{1}H NMR spectrum of MPESN-19-22 as a typical example. All of the aromatic protons are associated with the proposed copolymer structure, and the end-group peaks assignable to the telechelic oligomer disappear. The peaks around 1.73 and 2.05 ppm are assignable to the protons of methyl on the hydrophobic segments (k in Figure S3a, Supporting Information) and benzylmethyl groups on the hydrophilic segments (a in Figure S3a, Supporting Information), respectively. All three copolymers display a sufficiently high molecular weight for membrane formation (M_n > 60 kDa, as confirmed by GPC in Table 2).

Table 2. Molecular Weight, Polydispersity Index (M_w/M_n) and Degree of Bromination of MPESN

copolymer	M_w (Da)	M_n (Da)	M_w/M_n	bromination degree (%)
MPESN-9-22	101381	64365	1.5996	70.34
MPESN-19-22	112185	71846	1.6090	71.71
MPESN-30-22	134094	84629	1.5302	72.59

3.4. Synthesis and Characterization of Brominated Block Copolymers. The chemical structure and the degree of bromomethylation of the BrPESN were analyzed by ^{1}H NMR spectra. New peaks around 4.17−4.33 ppm assignable to the methylene protons of the bromomethyl groups are absent from the ^{1}H NMR spectrum of MPESN-19-22 (Figure S3a, Supporting Information), however, appear in that of BrPESN-19-22 (Figure S3b, Supporting Information). The peaks associated with the benzylmethyl groups (a in Figure S3, Supporting Information) decreased in size after bromomethylation. Successful synthesis of BrPESN-19-22 via bromination on MPESN-19-22 is thus confirmed. The degree of bromomethylation of the BrPESN, which can be calculated from the ratio of the integral area of the brominated benzyl peaks to (brominated benzyl peaks + unreacted benzylmethyl peaks), is in the range of 70−73%, as listed in Table 2.

3.5. Membrane Formation and FI-IR Spectrum. As depicted in Scheme 2, the ImPESN membranes were prepared using 1-methylimidazole as the functional agent and BrPESN as the base copolymers. The ^{1}H NMR spectrum of ImPESN-19-22 (Figure S4a, Supporting Information) shows the characteristic peaks of the methylene protons of the imidazolium ring at 9.13 ppm (H_1) and 7.9−8.0 ppm (H_2 and H_3) and methyl protons at around 3.6 ppm (H_4), indicating a successful introduction of the imidazolium groups into the AEMs. In addition, the characteristic peaks of Br−CH_2−Ar (Figure S3b, Supporting Information) shift almost completely downfield to 5.3 ppm for ImPESN-19-22 (Figure S4a, Supporting Information), which is assignable to the protons of N−CH_2−Ar.[11] This suggests that BrPESN converts mostly to ImPESN.

The successful synthesis of the copolymers and AEMs is further evidenced by FT-IR spectra (Figure S5, Supporting Information). The band at 2229 cm^{-1} is attributed to the symmetric stretching of nitrile groups, and the characteristic peak at 1244 cm^{-1} is assigned to phenoxy groups. For ImPESN-19-22, the characteristic peaks at 1636 and 737 cm^{-1} are attributed to the vibrational mode of imidazolium cations.[9] This confirms that 1-methylimidazole groups are successfully introduced into the ImPESN-19-22 membrane. The new broad absorption peak around 3404 cm^{-1} is attributed to the stretching vibrations of −OH bond. Both ^{1}H NMR and FT-IR confirm the structure of the ImPESN membranes.

3.6. Membrane Morphology. Figure 1 shows the appearance, SEM images of cross−section and surface of ImPESN-19-22. A transparent and flexible membrane can be observed from Figure 1a. The thickness of the membrane was observed to be 39 μm from Figure 1b. Figure 1c shows that the as−prepared membranes are homogeneous and dense without any visible flaws.

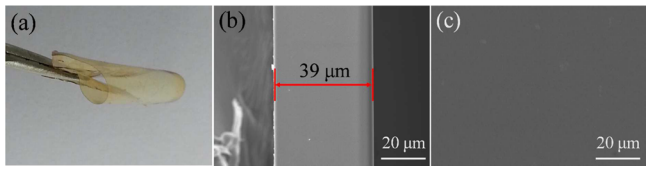

Figure 1. (a) Photo and (b) cross-sectional and (c) surface SEM images of ImPESN-19-22.

We further examined the morphology of the AEMs by AFM to investigate the hydrophilic/hydrophobic phase separation. Images of the AEM surfaces were recorded on the size scale of 500 × 500 nm in a tapping mode at ambient condition, as shown in Figure 2. The darker region in the phase image is assigned to the soft hydrophilic domain containing water, and the brighter region is associated with the hard hydrophobic backbones. As can be seen in Figure 2a−c, well-defined hydrophilic/hydrophobic phase separation is clearly observed in all of the as-prepared membranes. By increasing the hydrophilic block length, the AEMs exhibit larger hydrophilic domain size, as well as more pronounced and developed interconnectivity of ion domain.

DOI: 10.1021/acsami.5b01475
ACS Appl. Mater. Interfaces 2015, 7, 8284−8292

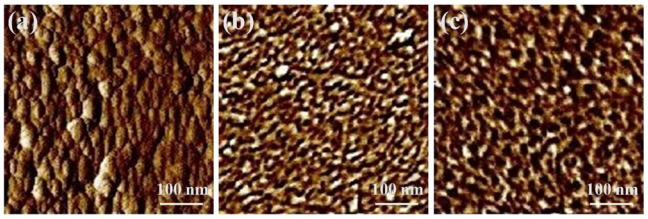

Figure 2. AFM phase images of (a) ImPESN-9-22, (b) ImPESN-19-22, and (c) ImPESN-30-22.

To gain a quantification of the ion domain, we also used SAXS to study the microphase-separated structure of the AEMs. As shown in Figure 3, obvious peaks are observed in the SAXS

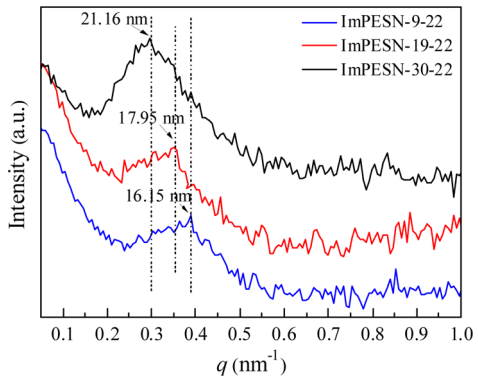

Figure 3. SAXS patterns of the AEMs.

spectra for all the ImPESN membranes. This indicates the generation of microphase separation between the hydrophilic and hydrophobic segments. The ionomer peaks are located at q_{max} = 0.389, 0.350, and 0.297 nm^{-1}. According to Bragg's law ($d = 2\pi/q_{max}$), the interdomain spacings (d) were calculated to be 16.15, 17.95, and 21.16 nm. These are associated with the size of the ion domains in the ImPESN membrane.[28] This result reveals that increasing the hydrophilic block length leads to an enlargement in the hydrophilic domain sizes, as confirmed by the AFM observation. The larger hydrophilic domains can form more developed interconnected ion−transport channels. The effects of morphological structure on the water uptake and ionic conductivity will be discussed later.

3.7. IEC, Water Uptake (WU), and Swelling Ratio of the Membranes. IEC represents the density of exchangeable groups in the membrane matrix. By increasing the hydrophilic block length, the IEC of the copolymers improved accordingly. As listed in Table 3, the IEC of the ImPESN membranes from ^{1}H NMR is in the range of 1.64−2.54 mequiv·g^{-1}, and the IEC from titration is about 1.58−2.43 mequiv·g^{-1}. The titrated IEC is in good agreement with that from ^{1}H NMR.

Water uptake and swelling ratio have a great effect on the ionic conductivity and mechanical property of AEMs. Water molecules can dissociate the alkali functionality and facilitate hydroxide ion transport. However, an excessive swelling induced by water uptake can also result in a poor dimensional stability and failure in mechanical strength. Therefore, maintaining the water uptake of AEMs at a suitable level is necessary to increase the ionic conductivity of the AEMs under the premise of ensuring mechanical strength.

As listed in Table 3, both the water uptake and the swelling ratio of the ImPESN membranes increased with increasing IEC and temperature. For example, by increasing the hydrophilic block length, the water uptake increased from 43.14 to 89.74% at 30 °C and from 53.92 to 106.84% at 60 °C, and the swelling ratio increased from 18.34 to 28.61% at 30 °C and from 23.19 to 39.40% at 60 °C. For a better comparison of the AEMs with different IECs, we calculated the number of absorbed water molecules per ion group (designated as λ). As shown in Table 3, λ for the ImPESN membranes is in the range of 15.15−20.49 at 30 °C and 18.94−24.40 at 60 °C.

A comparison with the multiblock[17,29] or random AEMs[30] currently reported in the literature is listed in Table 3, the ImPESN membranes with a similar IEC exhibited a higher water uptake and lower swelling. The reason for the ImPESN membranes with a comparatively high water uptake can be attributed to the formation of large and well-connected hydrophilic ion domains from the well-defined phase separation structure, as characterized by AFM and SAXS. The low swelling ratio indicates that the ImPESN membranes have good dimensional stability. This might be ascribed to the introduction of bulky and rigid PPH groups in the structure (Scheme 3). The bulky and rigid PPH groups suspended on the copolymer chains can force each chain apart to provide large interchain spacing in which the water molecules could be confined,[20] resulting in low swelling. Similar behavior was also observed in fluorene-containing AEMs and PEMs.[31,32] Furthermore, the presence of highly polar nitrile groups on the hydrophobic segments enhances the intra/intermolecular interaction in the copolymers and constrains swelling.[25,26]

3.8. Ionic Conductivity. As a critical property of AEMs, the ionic conductivity of the ImPESN membranes, as well as Nafion

Table 3. IEC, Water Uptake, λ, and Swelling Ratio of the AEMs

membrane	IEC (mequiv·g^{-1})		λ		WU (%)		SR (%)	
	calcd[a]	exptl[b]	30 °C	60 °C	30 °C	60 °C	30 °C	60 °C
ImPESN-9-22	1.64	1.58	43.14	53.92	15.15	18.94	18.34	23.19
ImPESN-19-22	2.15	2.07	68.45	86.40	18.35	23.16	25.47	33.38
ImPESN-30-22	2.54	2.43	89.74	106.84	20.49	24.40	28.61	39.40
Nafion 117[c]		0.89	21.34	28.63	13.32	17.87	19.69	25.22
QPPO−PAES−QPPO−0.76[d17]	1.96	1.60	33.0	37.6	11.5	13.1	22.7	25.1
QPPO−PAES−QPPO−1.14[d17]	2.43	1.83	53.0	64.2	16.1	19.5	31.1	38.0
APES−0.8[e29]	2.18	2.17	63.29	84.92	16.19	21.72	58.17	76.24
QAPEK−50[f30]	2.92	2.88	53	108	10.22	20.83	26.5	46

[a]Calculated from the ^{1}H NMR spectra. [b]Estimated by back-titration. [c]Measured under the same condition in our laboratory. [d]QPPO−PAES−QPPO: quaternized poly(2,6-dimethyl-1,4-phenylene oxide) and poly(arylene ether sulfone)s. [e]APES: quaternized fluorene-containing poly(arylene ether sulfone)s. [f]QAPEK: quaternary ammonium functionalized poly(arylene ether ketone)s.

DOI: 10.1021/acsami.5b01475
ACS Appl. Mater. Interfaces 2015, 7, 8284−8292

Scheme 3. Schematic Structure of the Multiblock Copolymer Chains

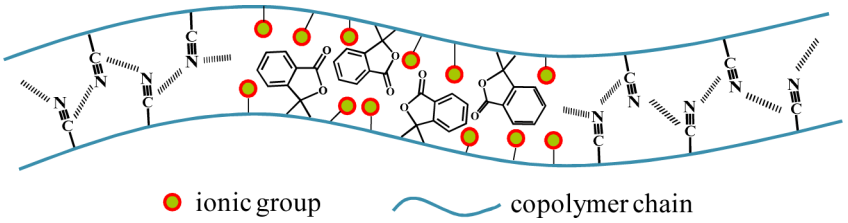

117, was measured in water as a function of temperature. As shown in Figure 4, the ionic conductivity of the ImPESN

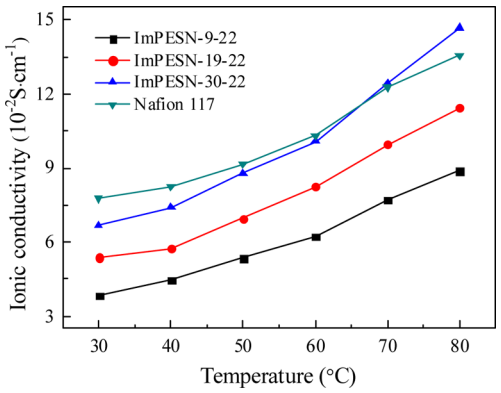

Figure 4. Temperature dependence of the ionic conductivity of the AEMs and Nafion 117.

membranes is in the range of 3.85−6.68 × 10^{-2} S·cm^{-1} at 30 °C and 8.90−14.67 × 10^{-2} S·cm^{-1} at 80 °C. It can be seen that the ionic conductivity increases with temperature because of the enhanced water mobility at elevated temperature. All the as-prepared AEMs show high ionic conductivities above the magnitude of 10^{-2} S·cm^{-1} over the temperature range. The conductivity also increases with increasing the hydrophilic block length. Furthermore, ImPESN-30-22 even shows a higher conductivity than Nafion 117 above 65 °C. The high conductivity can be attributed to the formation of effective ion transport pathways from the good phase-separated structure, as confirmed by AFM and SAXS. As shown above, the membranes with longer hydrophilic segments exhibited larger, more developed interconnected ion-conducting channels and higher water uptake. Those are favorable for higher conductivity.

3.9. Mechanical Properties. The mechanical property is another important parameter of the AEMs for the practical application of fuel cells. The mechanical properties of the ImPESN membranes were measured at RT and 60% RH, as shown in Table 4. The tensile strength of the as-prepared AEMs is in the range from 24.14 to 40.39 MPa, and the tensile elongation is in the range from 14.62 to 20.57%. The tensile strength and elongation depressed with increasing the length of hydrophilic block. This is probably due to that the longer hydrophilic block results in a higher water absorption and swelling of membranes. The water could act as a plasticizer[33] to depress the mechanical properties of the membranes.

Table 4. Mechanical Properties of the AEMs

membrane	tensile strength (MPa)	Young's modulus (MPa)	elongation at break (%)
ImPESN-9-22	40.39	336.59	20.57
ImPESN-19-22	31.68	265.43	17.28
ImPESN-30-22	24.14	230.76	14.62

3.10. Thermal Stability. The thermal stability of the ImPESN membranes in hydroxide form was investigated by TGA, as shown in Figure 5. It can be seen that all the AEMs

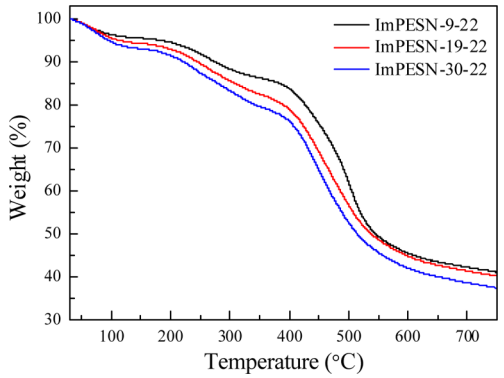

Figure 5. TGA curves of the AEMs under a nitrogen atmosphere.

exhibit a three−step decomposition behavior: (1) The first stage of slight degradation between 30 and 200 °C is due to the evaporation of the absorbed water and residual solvent (DMSO). (2) The second stage of degradation from 200 to 400 °C is assigned to the degradation of the imidazolium groups. (3) The third stage of degradation above 400 °C is attributed to the decomposition of the copolymer main chain. In general, all of the as-prepared ImPESN membranes exhibit good thermal stability below 200 °C. This suggests a good thermal stability of the ImPESN membranes for the application in AEMFCs.

3.11. Alkaline Stability. The alkaline stability of the ImPESN membranes was first evaluated by observing the changes in ionic conductivity after being soaked in a 2 M KOH solution at 60 °C. As shown in Figure 6, an initial sharp decrease

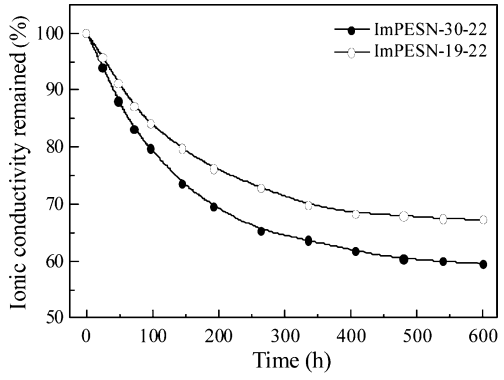

Figure 6. Alkaline stability of ImPESN-19-22 and ImPESN-30-22 in a 2 M KOH solution at 60 °C.

DOI: 10.1021/acsami.5b01475
ACS Appl. Mater. Interfaces 2015, 7, 8284−8292

in the ionic conductivity is within 300 h, after which the ionic conductivity tends to be a constant. After testing for 600 h, about 67% (3.62×10^{-2} S·cm^{-1}) and 59% (3.97×10^{-2} S·cm^{-1}) ionic conductivity remained for the ImPESN-19-22 and ImPESN-30-22 membranes, respectively. For a supplement, we also measured the change of the IEC of the AEMs. After the alkaline stability test, the IEC of ImPESN-19-22 and ImPESN-30-22 decreased from 2.07 to 1.61 mequiv·g^{-1} and from 2.43 to 1.70 mequiv·g^{-1}, respectively.

The membranes were further examined via ^{1}H NMR (Figure S4b, Supporting Information) and FT-IR (Figure S6, Supporting Information) after the alkaline stability test. The peak at 2232 cm^{-1} associated with the nitrile groups without a significant change suggests the integrity of the nitrile groups. Compared with the ^{1}H NMR (Figure S4a, Supporting Information) of ImPESN-19-22, a slight decrease in the intensity of the peaks (9.13, 8.0, 7.8, 5.3, 3.6 ppm) assignable to the imidazolium groups was observed after the alkaline stability test. This suggests the occurrence of degradation of the imidazolium groups. A negligible change around the aromatic proton area indicates the integrity of the polymer chain structures. All the results reveal that the ImPESN membranes have a moderate alkaline stability for the AEMFCs testing.

3.12. Single Cell Performance. The ImPESN-19-22 membrane is chosen for the single fuel cell test given it has good ionic conductivity and alkaline stability as well as sufficient mechanical strength. The polarization and power density–current density relationship curves are shown in Figure 7. An

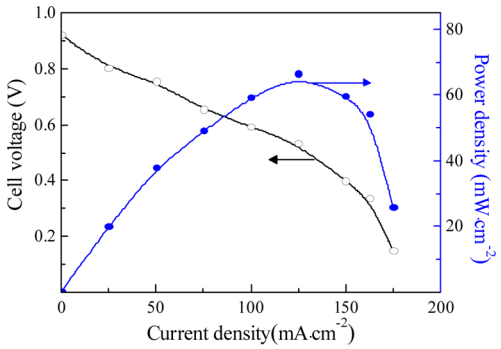

Figure 7. A single H_2/O_2 fuel cell performance using ImPESN-19-22 at 60 °C and 100% RH.

open circuit voltage (OCV) of 0.92 V and a peak power density of 66.4 mW·cm^{-2} at a current density of 125 mA·cm^{-2} can be achieved at 60 °C and 100% RH (Figure 7). This value is higher than that of the imidazolium functionalized random polysulfone AEMs at 60 °C (16 mW·cm^{-2}).[9] However, the peak power density is much lower than that of other high-performing H_2/O_2 fuel cells (Table 5). Besides the inherent character of the AEMs, the fuel cell performance is also affected by the MEA fabrication method, architecture of catalyst layer, and operating condition.[34−36] For this reason, further efforts will be devoted to optimizing these elements for better fuel cell performance.

4. CONCLUSIONS

A new series of phenolphthalein-based multiblock poly(arylene ether sulfone nitrile) AEMs were synthesized by block copolycondensation, bromination, imidazolium functionalizion, and alkalization. Combining both the benefits of the bulky aromatic structure of phenolphthalein groups on the hydrophilic segments and strongly polar nitrile groups on the hydrophobic segments, the ImPESN membranes show a well-defined phase-separated morphology to form ion-transport channels. The AEMs have good mechanical, thermal, and alkaline stability. The IEC of the AEMs is between 1.58 and 2.43 mequiv·g^{-1}. The water uptake varied in the range of 43.14−89.74% at 30 °C and 53.92−106.84% at 60 °C. Accordingly, the swelling ratio is 18.34−28.61% at 30 °C and 23.19−39.40% at 60 °C. The ionic conductivity of the membranes in the range of $3.85-14.67 \times 10^{-2}$ S·cm^{-1} increased with increasing hydrophilic block length and temperature. A single H_2/O_2 fuel cell testing using ImPESN-19-22 showed an open circuit voltage of 0.92 V and a maximum power density of 66.4 mW cm^{-2} at a current density of 125 mA·cm^{-2} at 60 °C. These results suggest that the ImPESN membranes are promising for AEMFCs applications.

■ ASSOCIATED CONTENT

Supporting Information

^{1}H NMR spectra of the DMPPH, oligomers, and copolymers; FT-IR and ^{1}H NMR spectra of ImPESN-19-22 before and after the alkaline stability test. This material is available free of charge via the Internet at http://pubs.acs.org.

■ AUTHOR INFORMATION

Corresponding Authors

*E-mail: qgzhang@xmu.edu.cn. Tel: 86-592-2188072. Fax: 86-592-2184822.

*E-mail: qlliu@xmu.edu.cn. Tel: 86-592-2188072. Fax: 86-592-2184822.

Notes

The authors declare no competing financial interest.

Table 5. Peak Power Density of H_2/O_2 AEMFC Reported in the Literature and This Work

AEM	temp (°C)	Pt loading (mg·cm^{-2})	ionomer	peak power density (mW·cm^{-2})
ImPESN-19-22 (this work)	60	1	ImPESN-30-22	66.4
PSf135-ImOH[a9]	60	2	PSf135-ImOH[a]	16
BIm-PPO-0.54[b11]	35	0.4	SION1[c]	13
qPVB/OH$^-$[d34]	15	0.8	qPVB/OH$^-$	156
TPQPOH152[e35]	70	0.2	TPQPOH124	258
ACDH96[f36]	50	0.4	AS-4[g]	370

[a]PSf-ImOH: imidazolium functionalized polysulfone. [b]BIm-PPO: benzimidazolium functionalized poly(phenylene oxide). [c]SION1: quaternized poly(vinylbenzyl chloride) using *N,N,N′,N′*-tetramethyl-1,6-hexanediamine. [d]qPVB/OH$^-$: quaternized poly(vinylbenzyl chloride). [e]TPQPOH: tris(2,4,6-trimethoxyphenyl)polysulfone-methylene quaternary phosphonium-hydroxide. [f]ACDH: cross-linked quaternized poly(vinybenzyl-divinylbenzene) bipolymer and the cross-linked quaternized poly(vinybenzyl-divinylbenzene-hexafluorobutyl methacrylate) terpolymer. [g]AS-4: purchased from Tokuyama Co.

DOI: 10.1021/acsami.5b01475
ACS Appl. Mater. Interfaces 2015, 7, 8284−8292

■ ACKNOWLEDGMENTS

Financial support from the National Nature Science Foundation of China (grant no. 21376194), the Nature Science Foundation of Fujian Province of China (grant no. 2014H0043), and the research fund for the Priority Areas of Development in Doctoral Program of Higher Education (no. 20130121130006) is gratefully acknowledged. We are very thankful for the referees' helpful comments.

■ REFERENCES

(1) Steele, B. C.; Heinzel, A. Materials for Fuel-Cell Technologies. *Nature* **2001**, *414*, 345−352.
(2) Zhang, H. W.; Shen, P. K. Recent Development of Polymer Electrolyte Membranes for Fuel Cells. *Chem. Rev.* **2012**, *112*, 2780−2832.
(3) Kreuer, K. D. Ion Conducting Membranes for Fuel Cells and Other Electrochemical Devices. *Chem. Mater.* **2014**, *26*, 361−380.
(4) Peighambardoust, S. J.; Rowshanzamir, S.; Amjadi, M. Review of the Proton Exchange Membranes for Fuel Cell Applications. *Int. J. Hydrogen Energy* **2010**, *35*, 9349−9384.
(5) Couture, G.; Alaaeddine, A.; Boschet, F.; Ameduri, B. Polymeric Materials as Anion-Exchange Membranes for Alkaline Fuel Cells. *Prog. Polym. Sci.* **2011**, *36*, 1521−1557.
(6) Merle, G.; Wessling, M.; Nijmeijer, K. Anion Exchange Membranes for Alkaline Fuel Cells: A Review. *J. Membr. Sci.* **2011**, *377*, 1−35.
(7) Xu, P. Y.; Zhou, K.; Han, G. L.; Zhang, Q. G.; Zhu, A. M.; Liu, Q. L. Effect of Fluorene Groups on the Properties of Multiblock Poly(arylene ether sulfone)s-Based Anion-Exchange Membranes. *ACS Appl. Mater. Interfaces* **2014**, *6*, 6776−6785.
(8) Tanaka, M.; Fukasawa, K.; Nishino, E.; Yamaguchi, S.; Yamada, K.; Tanaka, H.; Bae, B.; Miyatake, K.; Watanabe, M. Anion Conductive Block Poly(arylene ether)s: Synthesis, Properties, and Application in Alkaline Fuel Cells. *J. Am. Chem. Soc.* **2011**, *133*, 10646−10654.
(9) Zhang, F. X.; Zhang, H. M.; Qu, C. Imidazolium Functionalized Polysulfone Anion Exchange Membrane for Fuel Cell Application. *J. Mater. Chem.* **2011**, *21*, 12744−12752.
(10) Chen, D. Y.; Hickner, M. A. Degradation of Imidazolium- and Quaternary Ammonium-Functionalized Poly(fluorenyl ether ketone sulfone) Anion Exchange Membranes. *ACS Appl. Mater. Interfaces* **2012**, *4*, 5775−5781.
(11) Lin, X. C.; Liang, X. H.; Poynton, S. D.; Varcoe, J. R.; Ong, A. L.; Ran, J.; Li, Y.; Li, Q. H.; Xu, T. W. Novel Alkaline Anion Exchange Membranes Containing Pendant Benzimidazolium Groups for Alkaline Fuel Cells. *J. Membr. Sci.* **2013**, *443*, 193−200.
(12) Li, N. W.; Leng, Y. J.; Hickner, M. A.; Wang, C. Y. Highly Stable, Anion Conductive, Comb-Shaped Copolymers for Alkaline Fuel Cells. *J. Am. Chem. Soc.* **2013**, *135*, 10124−10133.
(13) Ye, Y. S.; Sharick, S.; Davis, E. M.; Winey, K. I.; Elabd, Y. A. High Hydroxide Conductivity in Polymerized Ionic Liquid Block Copolymers. *ACS Macro Lett.* **2013**, *2*, 575−580.
(14) Li, N. W.; Guiver, M. D. Ion Transport by Nanochannels in Ion-Containing Aromatic Copolymers. *Macromolecules* **2014**, *47*, 2175−2198.
(15) Yokota, N.; Ono, H.; Miyake, J.; Nishino, E.; Asazawa, K.; Watanabe, M.; Miyatake, K. Anion Conductive Aromatic Block Copolymers Containing Diphenyl Ether or Sulfide Groups for Application to Alkaline Fuel Cells. *ACS Appl. Mater. Interfaces* **2014**, *6*, 17044−17052.
(16) Disabb-Miller, M. L.; Johnson, Z. D.; Hickner, M. A. Ion Motion in Anion and Proton-Conducting Triblock Copolymers. *Macromolecules* **2013**, *46*, 949−956.
(17) Li, Q.; Liu, L.; Miao, Q. Q.; Jin, B. K.; Bai, R. K. Hydroxide-Conducting Polymer Electrolyte Membranes from Aromatic ABA Triblock Copolymers. *Polym. Chem.* **2014**, *5*, 2208−2213.
(18) Jasti, A.; Shahi, V. K. Multi-Block Poly(arylene ether)s Containing Pre-choloromethylated Bisphenol: Anion Conductive Ionomers. *J. Mater. Chem. A* **2013**, *1*, 6134−6137.
(19) Guo, R. L.; Lane, O.; VanHouten, D.; McGrath, J. E. Synthesis and Characterization of Phenolphthalein-Based Poly(arylene ether sulfone) Hydrophilic-Hydrophobic Multiblock Copolymers for Proton Exchange Membranes. *Ind. Eng. Chem. Res.* **2010**, *49*, 12125−12134.
(20) Zheng, J. F.; Wang, J.; Zhang, S. B.; Yuan, T.; Yang, H. Synthesis of Novel Cardo Poly(arylene ether sulfone)s with Bulky and Rigid Side Chains for Direct Methanol Fuel Cells. *J. Power Sources* **2014**, *245*, 1005−1013.
(21) Li, L.; Wang, Y. X. Quaternized Polyethersulfone Cardo Anion Exchange Membranes for Direct Methanol Alkaline Fuel Cells. *J. Membr. Sci.* **2005**, *262*, 1−4.
(22) Xiong, Y.; Liu, Q. L.; Zeng, Q. H. Quaternized Cardo Polyetherketone Anion Exchange Membrane for Direct Methanol Alkaline Fuel Cells. *J. Power Sources* **2009**, *193*, 541−546.
(23) Yun, S.; Parrondo, J.; Ramani, V. Derivatized Cardo-Polyetherketone Anion Exchange Membranes for All-Vanadium Redox Flow Batteries. *J. Mater. Chem. A* **2014**, *2*, 6605−6615.
(24) Zhang, Q.; Li, S. H.; Zhang, S. B. A Novel Guanidinium Grafted Poly(aryl ether sulfone) for High-Performance Hydroxide Exchange Membranes. *Chem. Commun.* **2010**, *46*, 7495−7497.
(25) Gao, Y.; Robertson, G. P.; Guiver, M. D.; Wang, G. Q.; Jian, X. G.; Mikhailenko, S. D.; Li, X.; Kaliaguine, S. Sulfonated Copoly-(phthalazinone ether ketone nitrile)s as Proton Exchange Membrane Materials. *J. Membr. Sci.* **2006**, *278*, 26−34.
(26) Li, Q.; Chen, Y.; Rowlett, J. R.; McGrath, J. E.; Mack, N. H.; Kim, Y. S. Controlled Disulfonated Poly(arylene ether sulfone) Multiblock Copolymers for Direct Methanol Fuel Cells. *ACS Appl. Mater. Interfaces* **2014**, *6*, 5779−5788.
(27) Sabnis, R. W. A Facile Synthesis of Phthalein Indicator Dyes. *Tetrahedron Lett.* **2009**, *50*, 6261−6263.
(28) Chen, D. Y.; Wang, S. J.; Xiao, M.; Meng, Y. Z.; Hay, A. S. Novel Polyaromatic Ionomers with Large Hydrophilic Domain and Long Hydrophobic Chain Targeting at Highly Proton Conductive and Stable Membranes. *J. Mater. Chem.* **2011**, *21*, 12068−12077.
(29) Xu, P. Y.; Zhou, K.; Han, G. L.; Zhang, Q. G.; Zhu, A. M.; Liu, Q. L. Fluorene-Containing Poly(arylene ether sulfone)s as Anion Exchange Membranes for Alkaline Fuel Cells. *J. Membr. Sci.* **2014**, *457*, 29−38.
(30) Chen, D. Y.; Hickner, M. A. Ion Clustering in Quaternary Ammonium Functionalized Benzylmethyl Containing Poly(arylene ether ketone)s. *Macromolecules* **2013**, *46*, 9270−9278.
(31) Rao, A. H. N.; Thankamony, R. L.; Kim, H. J.; Nam, S.; Kim, T. H. Imidazolium-Functionalized Poly(arylene ether sulfone) Block Copolymer as An Anion Exchange Membrane for Alkaline Fuel Cell. *Polymer* **2013**, *54*, 111−119.
(32) Bae, B.; Miyatake, K.; Uchida, M.; Uchida, H.; Sakiyama, Y.; Okanishi, T.; Watanabe, M. Sulfonated Poly(arylene ether sulfone ketone) Multiblock Copolymers with Highly Sulfonated Blocks. Long-Term Fuel Cell Operation and Post-Test Analyses. ACS. *ACS Appl. Mater. Interfaces* **2011**, *3*, 2786−2793.
(33) Dhakal, H. N.; Zhang, Z. Y.; Richardson, M. O. W. Effect of Water Absorption on the Mechanical Properties of Hemp Fibre Reinforced Unsaturated Polyester Composites. *Compos. Sci. Technol.* **2007**, *67*, 1674−1683.
(34) Cao, Y. C.; Wang, X.; Mamlouk, M.; Scott, K. Preparation of Alkaline Anion Exchange Polymer Membrane from Methylated Melamine Grafted Poly(vinylbenzyl chloride) and Its Fuel Cell Performance. *J. Mater. Chem.* **2011**, *21*, 12910−12916.
(35) Gu, S.; Cai, R.; Luo, T.; Jensen, K.; Contreras, C.; Yan, Y. S. Quaternary Phosphonium-Based Polymers as Hydroxide Exchange Membranes. *ChemSusChem* **2010**, *3*, 555−558.
(36) Zhao, Y.; Yu, H. M.; Xie, F.; Liu, Y. X.; Shao, Z. G.; Yi, B. L. High Durability and Hydroxide Ion Conducting Pore-Filled Anion Exchange Membranes for Alkaline Fuel Cell Applications. *J. Power Sources* **2014**, *269*, 1−6.

DOI: 10.1021/acsami.5b01475
ACS Appl. Mater. Interfaces 2015, 7, 8284−8292